Electronic Supplementary Information

Gigantic work function in layered AgF_2

W. Wegner,[1,2] K. Tokár[3,4], J. Lorenzana,[5] M. Derzsi,[2,3] W. Grochala[2]*

Contents.

S1. Computational methodology and determination of workfunction:

Projector-augmented-wave (PAW) method was applied[1,2] with rotationally invariant LSDA+U approach introduced by Liechtenstein *et al.*[3]. U and J values for Ag were set to be 5 eV and 1 eV, respectively, as it was previously applied for bulk AgF_2 [4,5]. Vienna Ab initio simulation package, VASP 5.4.1, was used for all computations[6–9].

AgF_2 bulk: Cut-off energy for plane wave basis set was set to E_{cut} = 520 eV. The blocked Davidson iteration scheme was used. Force, stress tensor, ions, cell shape and cell volume were relaxed. The energy convergence criterion (SCF) was set to 1 x 10^{-7} eV. The relaxations were stopped if all forces were smaller than 0.0003 eV/Å. Interpolation formula according to Vosko, Wilk and Nusair was used[10]. Gaussian smearing was used while ionic relaxation with conjugate gradient algorithm were performed. Tetrahedron method with Blöchl corrections were used for no update option. Smearing width was set to 0.04 eV. The k-point mesh of 12x12x12 was used for the magnetic cell identical with unit cell. The optimized lattice parameters of *P*bca cell 5.499 Å, 5.826 Å, and 5.056 Å match well the experimental values of 5.529 Å, 5.813 Å and 5.073 Å, respectively[11], discrepancies not exceeding 0.6%. Figure S2 shows calculated DOS for bulk system.

Unoptimized AgF_2 N-layer systems from the bulk: In order to calculate work function of AgF_2, N=1, 3, 5, 7, 9, 11 surface systems were constructed from preoptimized bulk AgF_2 with their geometry constrained to that found in a crystal. Unit cell were multiplied in the direction perpendicular to the layers to obtain the desired number of layers for further modelling, and to expose the (010) surface sheet towards the vacuum. Such choice of the surface is most natural since the inter-sheet interactions are weak leading to facile cleavage of the layers. *Ca.* 22.5 Å vacuum slab was added to obtained slabs (*cf.* SI for exemplary structure, Figure S1). Single point energies were calculated, followed by the density of states (with DOS evaluation at 3000 grid points) and the total local potential calculations. k-mesh in direction of added vacuum was reduced accordingly to preserve mesh density, with remaining parameters unchanged as compared to the bulk system. Exemplary DOS for N=9 system is showed at Figure S3.

Optimization of AgF_2 N=1 layer system: Geometry of the N = 1 AgF_2 layer system was optimized. The system was created by first cutting off the middle AgF_2 layer from the bulk structure. To prevent the collapse of the vacuum slab during optimization, the void was filled by adding helium atoms in the fractional (0, ½,0) and (½,½,½) sites. The distance between helium atoms was sufficiently large (over twice their van der Waals radius) to prevent their repulsion; in this way, small atoms of totally inert noble gas served as separator, which does not influence the crystal structure. After optimization, helium atoms were removed, and a vacuum slab was increased to ~12.5 Å while preserving the geometry of the AgF_2 single layer, and angles between unit cell vectors. So constructed system was used for calculation of the work function.

Optimization of hypothetical AgF_2 N=1 flat layer system: Geometry of the N = 1 hypothetical AgF_2 flat layer system was optimized. The preliminary structure model was similar to the one described above, albeit it was forced to be tetragonal, with F atoms placed in (½00) and (00½) positions. Similarly, to prevent the collapse of the vacuum slab during optimization, the void was filled by adding helium atoms in the fractional (0,½,0) and (½,½,½) sites. After optimization, helium atoms were removed, and a vacuum slab was increased to ~12.5 Å while preserving the geometry of the AgF_2 single flat layer.

AgF reference system:

Bulk AgF was optimized using DFT without spin polarization. The optimized lattice parameter of 4.88 Å matches the experimental value of 4.92 Å[12], discrepancy not exceeding *c.a.* 0.8%. After that N-layered systems for N=1,3, 5, 7, 9, 11 and exposing the (100) surface, were created using preoptimized bulk, and calculations with frozen geometries were performed. AgF slabs were separated with a vacuum one of *ca.* 22.5 Å.

Ag_2F reference system:
Bulk Ag_2F was optimized in the analogous manner as AgF. The optimized lattice parameter of a=b=2.945 Å and c=5.727 Å matches the experimental value of a=b=2.999 and c= 5.695 Å, discrepancy not exceeding 1.8% and 0.5%, respectively. After that N-layered systems for N=1, 3, 5, 7, 9, 11 and exposing the (001) surface (F terminals) were created in an analogous manner as for AgF, using preoptimized bulk, and calculations with frozen geometries were performed. Ag_2F Slabs were separated with a vacuum slab of *ca.* 22.5 Å.
Evaluation of work function:
The minimum work needed to remove one electron from an oriented slab occupied states to a remote point in vacuum is characterised by work function (W) defined by the difference[13]:

$$W = E_{vacuum} - E_F \qquad (Eq.1),$$

where (E_{vacuum}) is electrostatic potential in vacuum near surface as obtained from a maximum of planar averaged local electrostatic potential in supercell vacuum space between slab mirrors (determined using the VASP and P4VASP tool[14], and (E_F) is the Fermi level of the slab.

P4VASP and VESTA programs were used for drawings in this work[14,15]

S2. Reference system: N-surface NaF systems slabs from optimized bulk material:
Bulk NaF was optimized with the same parameters as for bulk AgF_2, using DFT without spin polarization. The optimized lattice parameter of 4.628 Å matches the experimental value of 4.619 Å[16], discrepancy not exceeding 0.2%. After that N-layered systems for N=3, 5, 7, 9, 11 and exposing the (100) surface were created in an analogous manner as for AgF_2, using preoptimized bulk, and calculations with frozen geometries were performed. Slabs were separated with a vacuum slab of *ca.* 24.5 Å. The same set of calculations were conducted for N-layered NaF systems as previously for unoptimized AgF_2 N-layered ones.

In Table S1 values obtained for NaF reference system are summarized. Here we see that with increasing thickness of the slab (N) values of E_{vacuum} and E_F are increasing. Work Function is rather stable and not dependent on slab thickness, and its value can be approximated to 6.7 eV.

Table S1. Results obtained from DFT calculation for not optimized N-layered systems of NaF build from optimized bulk material: Band Gap (BG), Vacuum energy (E_{vacuum}), Fermi Energy (E_F) and Work Function (W).

N	BG [eV]	E_{vacuum}	E_F	W
3	5.648	1.090	-5.580	6.671
5	5.719	1.560	-5.121	6.681
7	5.745	1.917	-4.766	6.683
9	5.761	2.198	-4.483	6.681
11	5.762	2.424	-4.262	6.686
bulk	5.553	---	-1.993	---

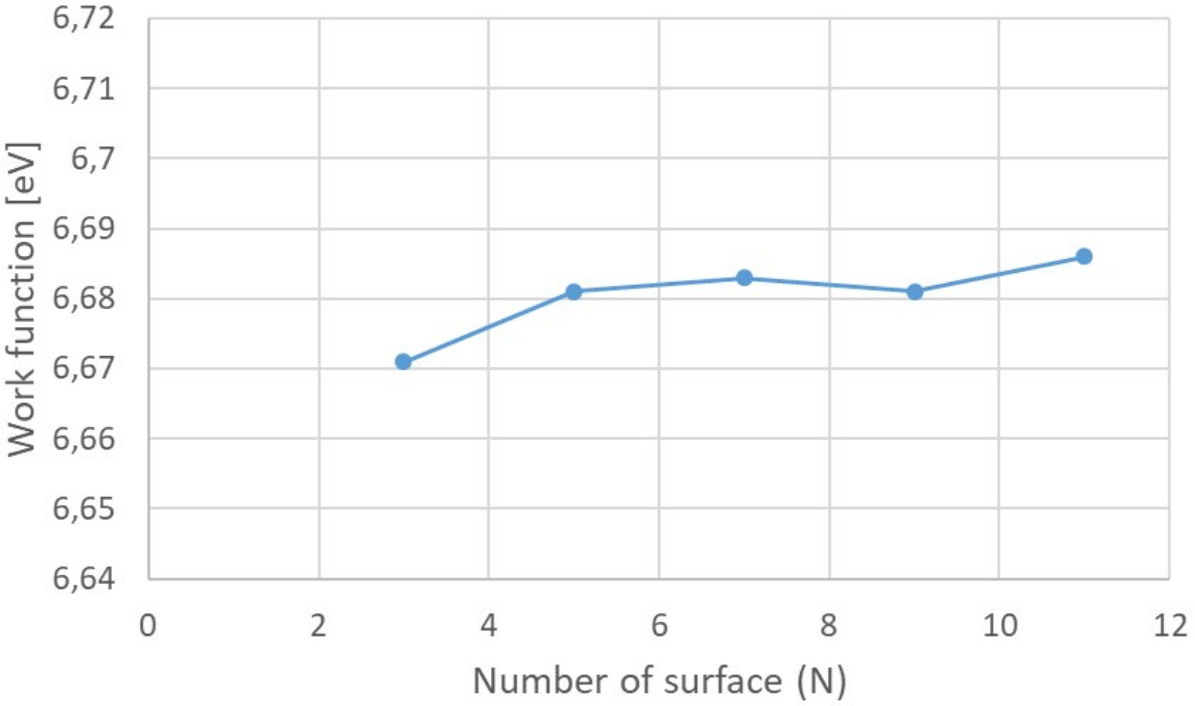

Figure S1. Work function for NaF.

S3. Reference system: N-surface AgF systems slabs from optimized bulk material:

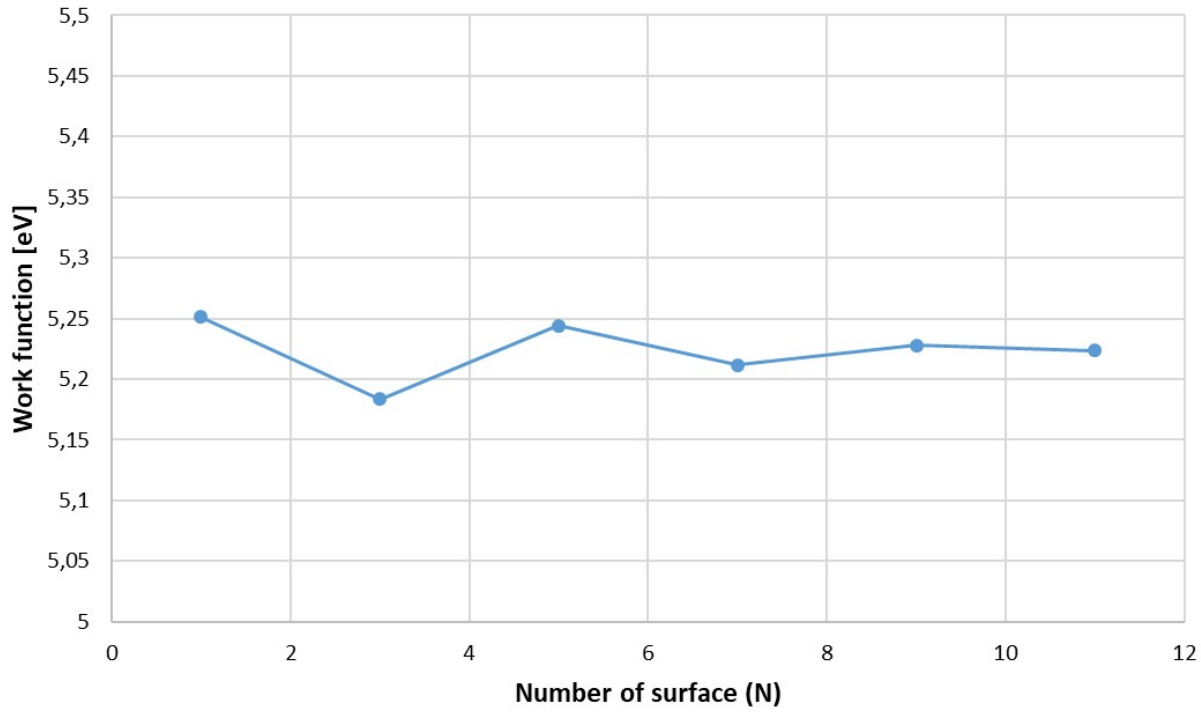

Figure S2. Work function for AgF.

Table S2. Results obtained from DFT calculation for not optimized N-layered systems of AgF build from optimized bulk material: Vacuum energy (E_{vacuum}), Fermi Energy (E_F) and Work Function (W).

N	E_{vacuum}	E_F	W
1	0.855	-4.396	5.251
3	2.136	-3.048	5.184
5	3.059	-2.185	5.244
7	3.742	-1.469	5.212
9	4.287	-0.941	5.228
11	4.719	-0.505	5.224

S4. Reference system: N-surface Ag_2F systems slabs from optimized bulk material:

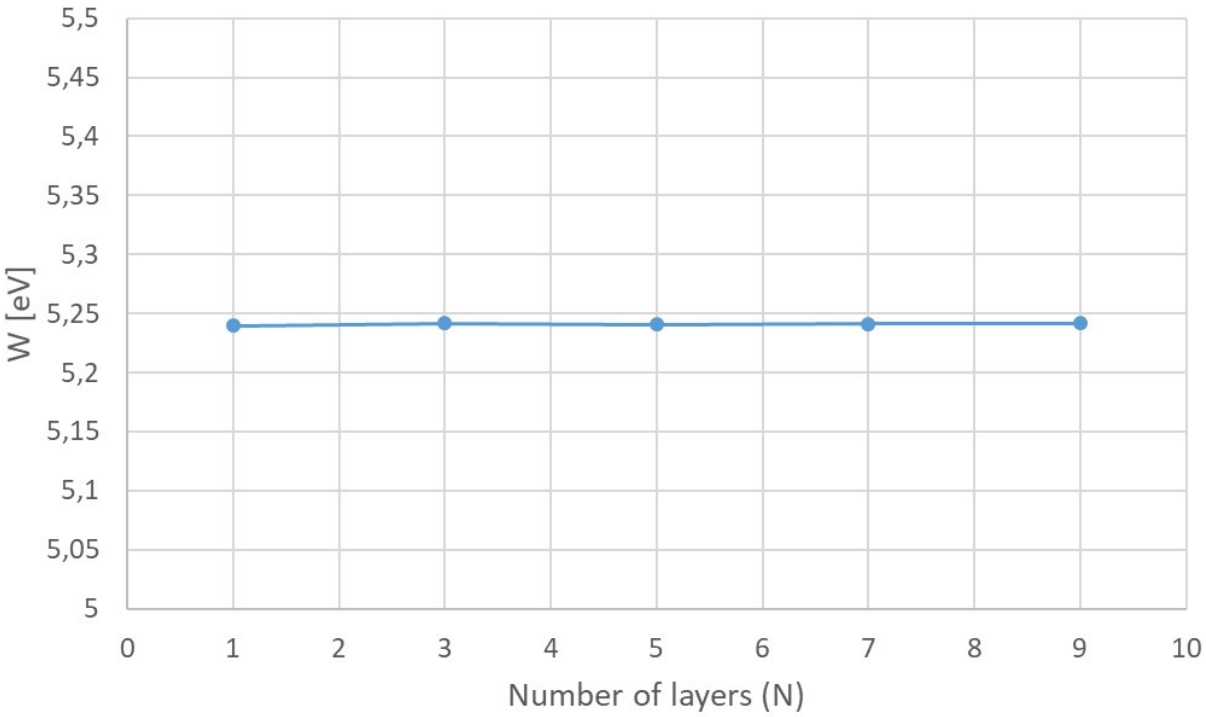

Figure S2. Work function for Ag_2F.

Table S3. Results obtained from DFT calculation for not optimized N-layered systems of NaF build from optimized bulk material: Band Gap (BG), Vacuum energy (E_{vacuum}), Fermi Energy (E_F) and Work Function (W).

N	E_{vacuum}	E_F	W
1	2.093	-3.147	5.240
3	4.639	-0.602	5.242
5	6.121	0.880	5.241
7	7.087	1.846	5.241
9	7.768	2.526	5.242

S5. Full DOS for relevant AgF_2 systems.

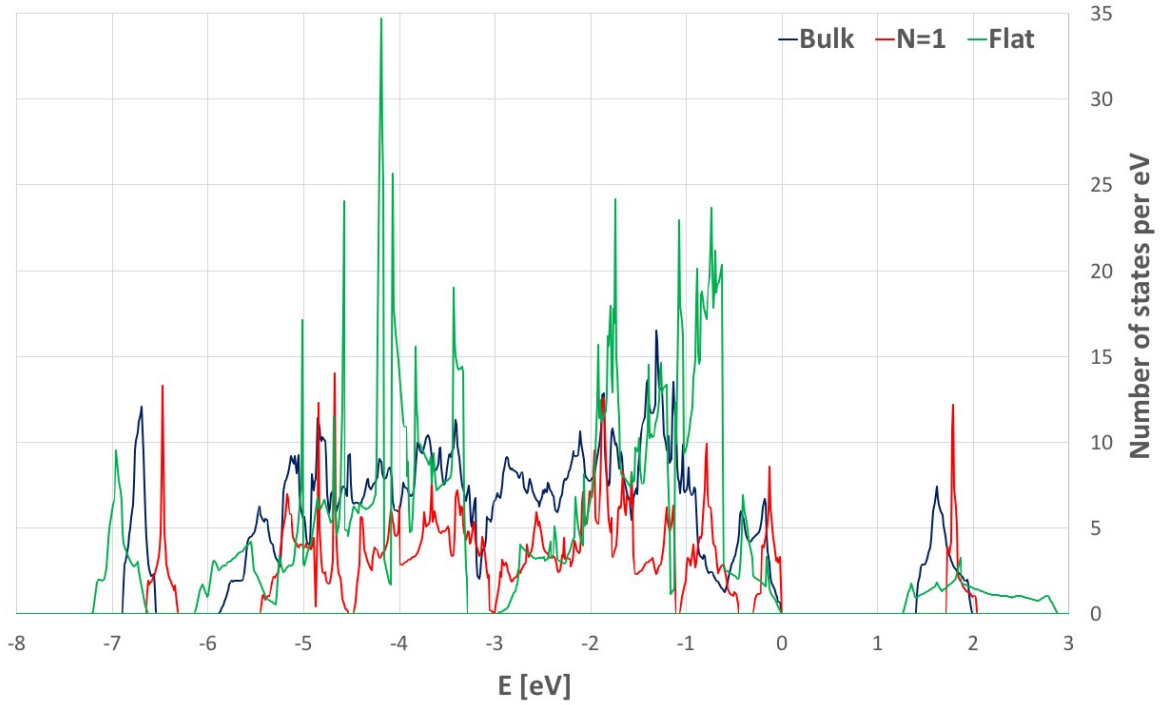

Full DOS is shown here to supplement information about the most relevant regions provided in the main text. One may easily notice that the absolute values of DOS are the largest for flat AgF_2 in several energy regions; this stems from the weakest mutual interactions of the Ag $d(z^2)$ orbitals which concomitantly result in a narrow band and high local DOS. Similar argument applies to the F p(z) orbitals. On the other hand, the orthogonal orbitals such as Ag $(x^2\text{-}y^2)$ or F p(x)/p(y) now interact most strongly among the three systems presented, which leads to substantial band dispersion and the smallest local DOS in the LHB & UHB, as discussed in the manuscript.

S6. Magnetic superexchange constant, J, in bulk AgF_2 and N=1 optimized system.

Magnetic superexchange in optimized single-layer as compared to bulk AgF_2 has been rationalized using previously published model [S17]. The angular dependence of J originates from the said reference. Now, two theoretical points from the current work have been overlaid; the filled blue triangle corresponds to computed AgF_2 structure in the bulk, while the empty triangle stands for the parameters calculated for an optimized single layer of AgF_2.
It may be seen that both points fit the theoretical dependence quite well. This factor alone suffices to state that large differences between the calculated Ag-F-Ag angles in the bulk and in an optimized single layer of AgF_2 allows us to explain the observed dramatic nearly 10-fold differences of J between these two structures.
On the other hand, the computed value for the flat layer system (ca. –200 meV) departs somewhat from that predicted by the model (of ca. –250 meV). However, the published model [S17] is valid only if U, charge transfer Δ, nearest neighbor repulsion, etc. remain the same. Since the flat layer form is characterized by the lack of apical fluorine, very large change in Δ as well as nearest neighbor repulsion are expected as compared to the bulk. Thus, the –200 vs. –250 meV discrepancy may rather easily be justified.

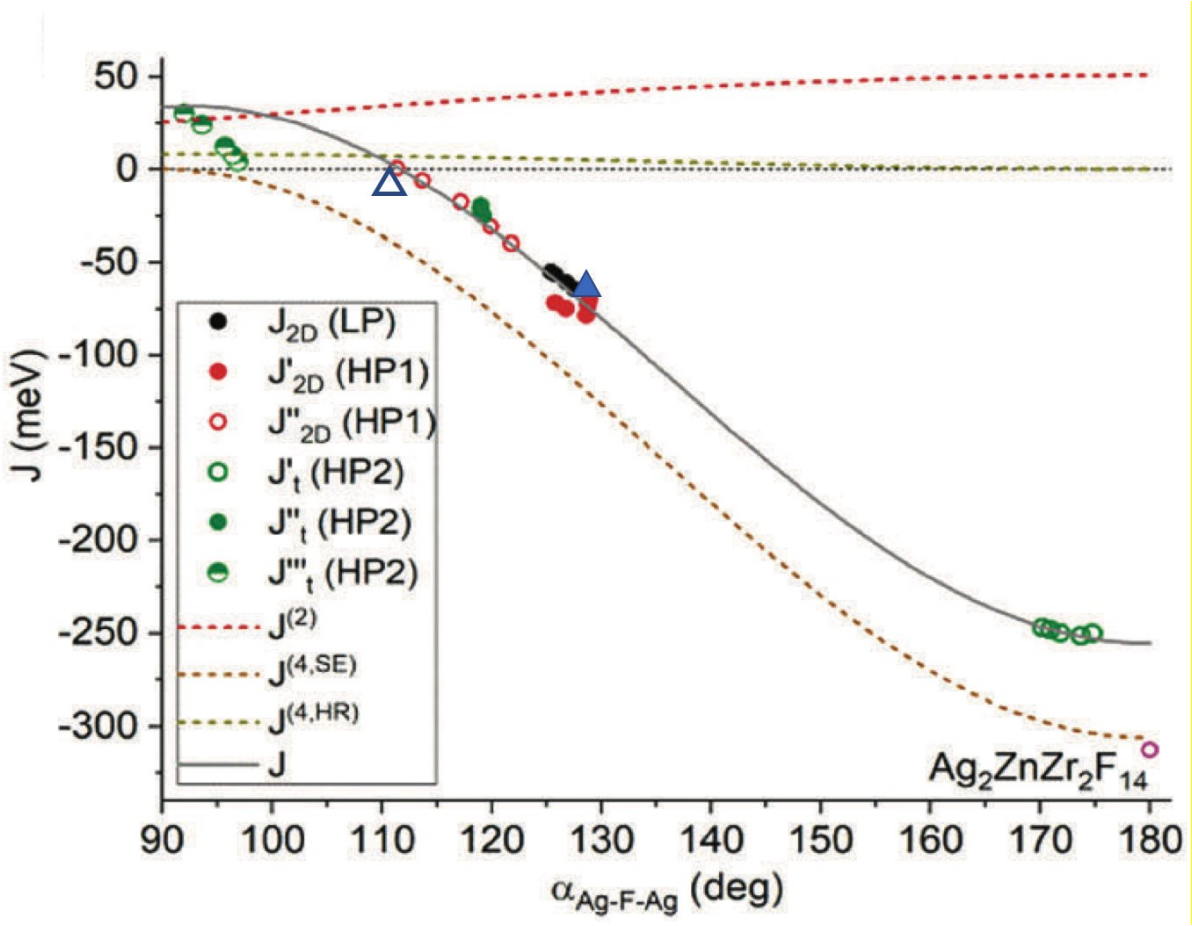

S7. Crystallographic Information Files.

CIF file for bulk AgF_2 optimized system:

#==

CRYSTAL DATA

#--

data_AgF2_Bulk

_chemical_name_common ''
_cell_length_a 5.49911
_cell_length_b 5.82599
_cell_length_c 5.05574
_cell_angle_alpha 90
_cell_angle_beta 90
_cell_angle_gamma 90
_space_group_name_H-M_alt 'P 1'
_space_group_IT_number 1

loop_

```
_space_group_symop_operation_xyz
   'x, y, z'

loop_
   _atom_site_label
   _atom_site_occupancy
   _atom_site_fract_x
   _atom_site_fract_y
   _atom_site_fract_z
   _atom_site_adp_type
   _atom_site_B_iso_or_equiv
   _atom_site_type_symbol
   Ag1       1.0    0.000000    -0.000000     0.000000    Biso  1.000000 Ag
   Ag2       1.0    0.500000     0.000000     0.500000    Biso  1.000000 Ag
   Ag3       1.0    0.000000     0.500000     0.500000    Biso  1.000000 Ag
   Ag4       1.0    0.500000     0.500000     0.000000    Biso  1.000000 Ag
   F1        1.0    0.305732     0.868176     0.183685    Biso  1.000000 F
   F2        1.0    0.694268     0.131824     0.816315    Biso  1.000000 F
   F3        1.0    0.194268     0.131824     0.683685    Biso  1.000000 F
   F4        1.0    0.805732     0.868176     0.316315    Biso  1.000000 F
   F5        1.0    0.694268     0.368176     0.316315    Biso  1.000000 F
   F6        1.0    0.305732     0.631824     0.683685    Biso  1.000000 F
   F7        1.0    0.805732     0.631824     0.816315    Biso  1.000000 F
   F8        1.0    0.194268     0.368176     0.183685    Biso  1.000000 F
```

CIF file for N=1 layer AgF_2 optimized system:

```
#======================================================================

# CRYSTAL DATA

#----------------------------------------------------------------------

data_AgF2_1N


_chemical_name_common                  ''
_cell_length_a                         5.72758
_cell_length_b                         25.08496
_cell_length_c                         3.72589
_cell_angle_alpha                      90
_cell_angle_beta                       90
_cell_angle_gamma                      74.49773
_space_group_name_H-M_alt              'P 1'
_space_group_IT_number                 1

loop_
_space_group_symop_operation_xyz
   'x, y, z'
```

```
loop_
  _atom_site_label
  _atom_site_occupancy
  _atom_site_fract_x
  _atom_site_fract_y
  _atom_site_fract_z
  _atom_site_adp_type
  _atom_site_B_iso_or_equiv
  _atom_site_type_symbol
  Ag1      1.0    0.000000     0.125000     0.500000    Biso  1.000000 Ag
  Ag2      1.0    0.500000     0.125000     0.000000    Biso  1.000000 Ag
  F1       1.0    0.728499     0.086095     0.407047    Biso  1.000000 F
  F2       1.0    0.271501     0.163905     0.592953    Biso  1.000000 F
  F3       1.0    0.771501     0.163905     0.907047    Biso  1.000000 F
  F4       1.0    0.228499     0.086095     0.092953    Biso  1.000000 F
```

CIF file for N=1 layer AgF_2 optimized tetragonal flat layer system:

```
#======================================================================

# CRYSTAL DATA

#----------------------------------------------------------------------

data_AgF2_1Nflat


_chemical_name_common                  ''
_cell_length_a                         8.04142
_cell_length_b                         25.58947
_cell_length_c                         8.04037
_cell_angle_alpha                      90
_cell_angle_beta                       90
_cell_angle_gamma                      90
_space_group_name_H-M_alt              'P 1'
_space_group_IT_number                 1

loop_
_space_group_symop_operation_xyz
   'x, y, z'

loop_
  _atom_site_label
  _atom_site_occupancy
  _atom_site_fract_x
  _atom_site_fract_y
  _atom_site_fract_z
  _atom_site_adp_type
  _atom_site_B_iso_or_equiv
  _atom_site_type_symbol
```

```
  Ag1      1.0    0.000000     0.109214     0.000000    Biso  1.000000 Ag
  Ag2      1.0    0.000000     0.109214     0.500000    Biso  1.000000 Ag
  Ag3      1.0    0.500000     0.109214     0.000000    Biso  1.000000 Ag
  Ag4      1.0    0.500000     0.109214     0.500000    Biso  1.000000 Ag
  F1       1.0    0.250000     0.109214     0.000000    Biso  1.000000 F
  F2       1.0    0.250000     0.109214     0.500000    Biso  1.000000 F
  F3       1.0    0.750000     0.109214     0.000000    Biso  1.000000 F
  F4       1.0    0.750000     0.109214     0.500000    Biso  1.000000 F
  F5       1.0    0.000000     0.109214     0.250000    Biso  1.000000 F
  F6       1.0    0.000000     0.109214     0.750000    Biso  1.000000 F
  F7       1.0    0.500000     0.109214     0.250000    Biso  1.000000 F
  F8       1.0    0.500000     0.109214     0.750000    Biso  1.000000 F
```

CIF file for N=11 layer AgF_2 unoptimized system:

```
#======================================================================

# CRYSTAL DATA

#----------------------------------------------------------------------

data_AgF2_N11


_chemical_name_common                  ' '
_cell_length_a                         5.49911
_cell_length_b                         54.95596
_cell_length_c                         5.05574
_cell_angle_alpha                      90
_cell_angle_beta                       90
_cell_angle_gamma                      90
_space_group_name_H-M_alt              'P 1'
_space_group_IT_number                 1

loop_
_space_group_symop_operation_xyz
   'x, y, z'

loop_
   _atom_site_label
   _atom_site_occupancy
   _atom_site_fract_x
   _atom_site_fract_y
   _atom_site_fract_z
   _atom_site_adp_type
   _atom_site_B_iso_or_equiv
   _atom_site_type_symbol
   Ag1      1.0    0.000000     0.106012     0.000000    Biso  1.000000 Ag
   Ag2      1.0    0.000000     0.212024     0.000000    Biso  1.000000 Ag
   Ag3      1.0    0.000000     0.318036     0.000000    Biso  1.000000 Ag
```

Ag4	1.0	0.000000	0.424048	0.000000	Biso	1.000000	Ag
Ag5	1.0	0.000000	0.530060	0.000000	Biso	1.000000	Ag
Ag6	1.0	0.500000	0.106012	0.500000	Biso	1.000000	Ag
Ag7	1.0	0.500000	0.212024	0.500000	Biso	1.000000	Ag
Ag8	1.0	0.500000	0.318036	0.500000	Biso	1.000000	Ag
Ag9	1.0	0.500000	0.424048	0.500000	Biso	1.000000	Ag
Ag10	1.0	0.500000	0.530060	0.500000	Biso	1.000000	Ag
Ag11	1.0	0.000000	0.053006	0.500000	Biso	1.000000	Ag
Ag12	1.0	0.000000	0.159018	0.500000	Biso	1.000000	Ag
Ag13	1.0	0.000000	0.265030	0.500000	Biso	1.000000	Ag
Ag14	1.0	0.000000	0.371042	0.500000	Biso	1.000000	Ag
Ag15	1.0	0.000000	0.477054	0.500000	Biso	1.000000	Ag
Ag16	1.0	0.000000	0.583066	0.500000	Biso	1.000000	Ag
Ag17	1.0	0.500000	0.053006	0.000000	Biso	1.000000	Ag
Ag18	1.0	0.500000	0.159018	0.000000	Biso	1.000000	Ag
Ag19	1.0	0.500000	0.265030	0.000000	Biso	1.000000	Ag
Ag20	1.0	0.500000	0.371042	0.000000	Biso	1.000000	Ag
Ag21	1.0	0.500000	0.477054	0.000000	Biso	1.000000	Ag
Ag22	1.0	0.500000	0.583066	0.000000	Biso	1.000000	Ag
F1	1.0	0.305732	0.092037	0.183685	Biso	1.000000	F
F2	1.0	0.305732	0.198049	0.183685	Biso	1.000000	F
F3	1.0	0.305732	0.304061	0.183685	Biso	1.000000	F
F4	1.0	0.305732	0.410073	0.183685	Biso	1.000000	F
F5	1.0	0.305732	0.516085	0.183685	Biso	1.000000	F
F6	1.0	0.694268	0.119987	0.816315	Biso	1.000000	F
F7	1.0	0.694268	0.225999	0.816315	Biso	1.000000	F
F8	1.0	0.694268	0.332011	0.816315	Biso	1.000000	F
F9	1.0	0.694268	0.438023	0.816315	Biso	1.000000	F
F10	1.0	0.694268	0.544035	0.816315	Biso	1.000000	F
F11	1.0	0.194268	0.119987	0.683685	Biso	1.000000	F
F12	1.0	0.194268	0.225999	0.683685	Biso	1.000000	F
F13	1.0	0.194268	0.332011	0.683685	Biso	1.000000	F
F14	1.0	0.194268	0.438023	0.683685	Biso	1.000000	F
F15	1.0	0.194268	0.544035	0.683685	Biso	1.000000	F
F16	1.0	0.805732	0.092037	0.316315	Biso	1.000000	F
F17	1.0	0.805732	0.198049	0.316315	Biso	1.000000	F
F18	1.0	0.805732	0.304061	0.316315	Biso	1.000000	F
F19	1.0	0.805732	0.410073	0.316315	Biso	1.000000	F
F20	1.0	0.805732	0.516085	0.316315	Biso	1.000000	F
F21	1.0	0.694268	0.039031	0.316315	Biso	1.000000	F
F22	1.0	0.694268	0.145043	0.316315	Biso	1.000000	F
F23	1.0	0.694268	0.251055	0.316315	Biso	1.000000	F
F24	1.0	0.694268	0.357067	0.316315	Biso	1.000000	F
F25	1.0	0.694268	0.463079	0.316315	Biso	1.000000	F
F26	1.0	0.694268	0.569091	0.316315	Biso	1.000000	F
F27	1.0	0.305732	0.066981	0.683685	Biso	1.000000	F
F28	1.0	0.305732	0.172993	0.683685	Biso	1.000000	F
F29	1.0	0.305732	0.279005	0.683685	Biso	1.000000	F
F30	1.0	0.305732	0.385017	0.683685	Biso	1.000000	F
F31	1.0	0.305732	0.491029	0.683685	Biso	1.000000	F

F32	1.0	0.305732	0.597041	0.683685	Biso	1.000000 F
F33	1.0	0.805732	0.066981	0.816315	Biso	1.000000 F
F34	1.0	0.805732	0.172993	0.816315	Biso	1.000000 F
F35	1.0	0.805732	0.279005	0.816315	Biso	1.000000 F
F36	1.0	0.805732	0.385017	0.816315	Biso	1.000000 F
F37	1.0	0.805732	0.491029	0.816315	Biso	1.000000 F
F38	1.0	0.805732	0.597041	0.816315	Biso	1.000000 F
F39	1.0	0.194268	0.039031	0.183685	Biso	1.000000 F
F40	1.0	0.194268	0.145043	0.183685	Biso	1.000000 F
F41	1.0	0.194268	0.251055	0.183685	Biso	1.000000 F
F42	1.0	0.194268	0.357067	0.183685	Biso	1.000000 F
F43	1.0	0.194268	0.463079	0.183685	Biso	1.000000 F
F44	1.0	0.194268	0.569091	0.183685	Biso	1.000000 F

S8. References:

[1] P. E. Blochl, *Phys. Rev. B* **1994**, *50*, 17953.
[2] G. Kresse, D. Joubert, *Phys. Rev. B* **1999**, *59*, 1758.
[3] A. I. Liechtenstein, V. I. Anisimov, J. Zaanen, *Phys. Rev. B* **1995**, *52*, R5467.
[4] A. Grzelak, J. Gawraczyński, T. Jaroń, D. Kurzydłowski, A. Budzianowski, Z. Mazej, P. J. Leszczyński, V. B. Prakapenka, M. Derzsi, V. V. Struzhkin, et al., *Inorg. Chem.* **2017**, *56*, 14651–14661.
[5] M. Derzsi, A. Grzelak, P. Kondratiuk, K. Tokár, W. Grochala, *Crystals* **2019**, *9*, 423.
[6] G. Kresse, J. Hafner, *Phys. Rev. B* **1993**, *47*, 558.
[7] G. Kresse, J. Hafner, *Phys. Rev. B* **1994**, *49*, 14251.
[8] G. Kresse, J. Furthmü, *Phys. Rev. B* **1996**, *54*, 11169.
[9] G. Kresse, J. Furthmüller, *Comput. Mater. Sci.* **1996**, *6*, 15–50.
[10] S. H. Vosko, L. Wilk, M. Nusair, *Accurate Spin-Dependent Electron Liquid Correlation Energies for Local Spin Density Calculations: A Critical Analysis*, **1980**.
[11] P. Fischer, D. Schwarzenbach, H. M. Rietveld, *J. Phys. Chem. Solids* **1971**, *32*, 543–550.
[12] R. Breslow New York, N. York Hai Won Chang, *) A. Sieverts and H. Moritz*, UTC, **1930**.
[13] N. E. Singh-Miller, N. Marzari, *Phys. Rev. B* **2009**, *80*, 235407.
[14] O. Dubay, "No Title," **n.d.**
[15] K. Momma, F. Izumi, *J. Appl. Crystallogr.* **2011**, *44*, 1272–1276.
[16] M. Liao, Y. Zang, Z. Guan, H. Li, Y. Gong, K. Zhu, X. P. Hu, D. Zhang, Y. Xu, Y. Y. Wang, et al., *Nat. Phys.* **2018**, *14*, 344–348.
[17] D. Kurzydłowski, M. Derzsi, P. Barone, A. Grzelak, V. V. Struzhkin, J. Lorenzana, W. Grochala, *Chem. Commun.* **2018**, *54*, 10252–10255.
[18] A. Grzelak, H. Su, X. Yang, D. Kurzydłowski, J. Lorenzana, W. Grochala, *Phys. Rev. Mater.* **2020**, *4*, 084405.